Results in Physics 10 (2018) 727–730

Contents lists available at ScienceDirect

Results in Physics

journal homepage: www.elsevier.com/locate/rinp

Nano-capacitor-like model using light trapping in plasmonic island embedded microring system

J. Ali[a], P. Youplao[b], N. Pornsuwancharoen[b], M.A. Jalil[c], S. Chiangga[d], I.S. Amiri[e], S. Punthawanunt[f], M.S. Aziz[a], G. Singh[g], P. Yupapin[h,i,*], K.T.V. Grattan[j]

[a] Laser Centre, IBNU SINA ISIR, Universiti Teknologi Malaysia, 81310 Johor Bahru, Malaysia
[b] Department of Electrical Engineering, Faculty of Industry and Technology, Rajamangala University of Technology Isan, Sakon Nakhon Campus, 199 Phungkon, Sakon Nakhon 47160, Thailand
[c] Physics Department, Faculty of Science, Universiti Teknologi Malaysia, 81310 Johor Bahru, Malaysia
[d] Department of Physics, Faculty of Science, Kasetsart University, Bangkok 10900, Thailand
[e] Division of Materials Science and Engineering, Boston University, Boston, MA 02215, USA
[f] Multidisciplinary Research Center, Faculty of Science and Technology, Kasem Bundit University, Bangkok 10250, Thailand
[g] Department of Electronics and Communication Engineering, Malaviya National Institute of Technology Jaipur, 302017, India
[h] Computational Optics Research Group, Advanced Institute of Materials Science, Ton Duc Thang University, District 7, Ho Chi Minh City, Viet Nam
[i] Faculty of Electrical & Electronics Engineering, Ton Duc Thang University, District 7, Ho Chi Minh City, Viet Nam
[j] Department of Electrical & Electronic Engineering, School of Mathematics, Computer Science & Engineering, City, University of London, EC1V 0HB, United Kingdom

ABSTRACT

We have proposed the convincing electro-optic circuit for long life-time electron mobility emission. Light a monochromatic source is utilized as input into the circuit via the input port and trapped within the plasmonic island. It is a formed-like capacitor structure formed by the silicon-graphene-gold materials which are stacked layers. All circuit port ends have added the TiO_2 to form the reflectors. By selecting the suitable parameters, the fraction of the output power emission can be controlled at the add port, from which it can be successively pumping and trapped(stored) within the plasmonic island. The system energy saturation can be released by squeezing light behavior, therefore, the system is always balanced due to the successive pumping process. The results obtained of the single cell(circuit) have shown that the charging time and discharging times of the nano-capacitor-like of ~2 to 3 s and 1000 h are achieved. This can be applied to long life mobility emission (discharge) of the capacity-like device. The mobility storage time within the island is 14,000 h, with the electron mobility of $\sim \mathbf{3.0} \times \mathbf{10^{-7}}\ \mathbf{cm^2\ Vs^{-1}}$ is obtained.

Introduction

Light trapping within a micro-scale device has become the promising technique for various applications, where there are many types of research and investigations in various investigations [1–5]. Energy storage using the light trapping technique is also the interesting method for long life power emission. Many works in both theory and practice have been reported [6–11], where there were different trapping systems applied. The key advantage of them is the tiny trapping system with the suitable materials could offer different applications. Light trapping within a microring system is also the interesting technique for energy storage [12], in which the electro-optic energy conversion can be formed and used for battery [13]. The electro-optic conversion can be formed by using the device called the plasmonic island and stacked layers, in which light energy can be converted to be the electron mobility and current, which can be used as the charge and discharge current for battery applications. Principally, the light intensity can be converted to be the electron mobility by using the following relationship as $\boldsymbol{I} = \boldsymbol{E}^2 = \left(\frac{V_d}{\mu}\right)^2$. Here, the light intensity is presented by *I*, and the group velocity is defined as $V_d = \mu E$. An electric current can be established in the conductor once an electric field of *E* is applied in the grating sensor, where the current density can be defined as $J_s = \sigma E$. Here, the conductance or the electrical conductivity is defined by σ, where for the gold material it is $1.6 \times 10^8\,W^{-1}\,m^{-1}$ [14,15]. By modifying the microring resonator design as add-drop filter consisting of two microring resonators attached to the centred ring, we can induce the nonlinear effects to the system which offers a generation of short pulses and easy control of the WGM resonance output compared with the original microring resonator design [16–18]. The sensitivity of the system can be obtained by the relationship between the electron mobility output and the applied current (input power). By using the plasmonic island, the plasmonic waves are introduced in the graphene layer by the input light intensity from the silicon layer, from which the

* Corresponding author at: Computational Optics Research Group, Advanced Institute of Materials Science, Ton Duc Thang University, District 7, Ho Chi Minh City, Viet Nam.
E-mail address: preecha.yupapin@tdt.edu.vn (P. Yupapin).

https://doi.org/10.1016/j.rinp.2018.07.013
Received 4 June 2018; Accepted 13 July 2018
Available online 21 July 2018

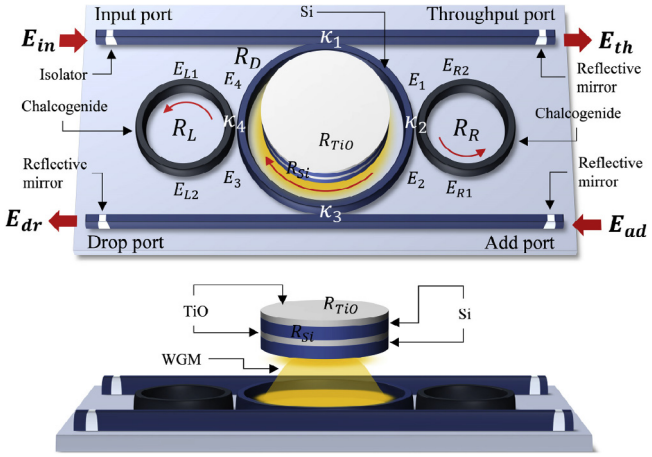

Fig. 1. Schematic of a plasmonic island structure, where E_{in}, E_{th}, E_{dr}, E_{ad} are the electrical fields of the input, through, drop and add ports, R_L, R_R, R_D are the ring radii of the left, right, and center ring, respectively, κ_s : the coupling coefficients are 0.5. Si: Silicon, R_{si}: Silicon ring radius, R_{TiO}: Titanium oxide circle radius.

electron mobility is driven by the surface plasmon waves. The excited electrons are conducted within the gold layer by the driven plasmonic waves. In this article, the trapping light within the Panda-ring circuit is controlled to have the low-emission rate by the applied reflector length (coefficient). The silicon device on-chip with the scale less than 1 μm has been recently reported, however, this work the device is formed by the ChG microring structure, in which the device scale is proposed by the practical fabrication scale [19]. The low energy(electron mobility) emission is configured by the black-body-radiation. The system is fed by the external energy, then it is almost closed during the operation.

The generated electro-optic signal conversion within the system in Fig. 1 can be obtained by the relationship between the plasmon wave energy and electron mobility within the gold layer [20]. The driven group velocity within the device can generate the required WGM beam output. By adjusting the input power and also the phase modulator which is realized as two nonlinear ring sides, the whispering gallery mode can be controlled. Suitable pumping power can be applied to the center wavelength signal and the resonant pulse width by using the nonlinear materials such as ZnO. Here, the resonance pulse width is defined as switching time. Eq. (1) representing the electrical output field ($\mathbf{E_{WGM}}$) in the cylindrical coordinator [17]. To simplify the equation, the surface reflection of the reflector is neglected, where $\mathbf{I_{WGMR}} = -\mathbf{R_{WGM}}\ \mathbf{I_{WGMR}}$. $\mathbf{R_{WGM}}$ which is the reflection output. Here, $\mathbf{R_{WGM}}$, is the reflection coefficient or the reflectivity of the used material [21]. Further investigations can be performed by using different filters, as the output from the circuit can interfere with the reflection power, where the results from the interference output can be detected and seen in the output ports of the system. To obtain such interference results we have selected simulation system parameters from experimental works [22,23]. The used parameters are given in the captions of relevant figures. In Fig. 1, a selected light source is fed into the system via an input port, which is represented as the input electric field ($\boldsymbol{E_{in}}$). The electric fields are circulated within the system and described by the Eqs. (1)–(3) [21], the input electric field is fed into the z-axis, where $\boldsymbol{E_{in}} = \boldsymbol{E_Z} = \boldsymbol{E_0 e^{-ik_z - \omega t + \varphi}}$, $\boldsymbol{E_0}$ is the initial electric field amplitude, Where $\boldsymbol{E_0}$ is the electric field amplitude (real), $\boldsymbol{k_z}$ is the wave number in the direction of propagation (z-axis) and $\boldsymbol{\omega}$ is the angular frequency, where $\boldsymbol{\varphi}$ is the phase of light.

$$E_{th} = \sqrt{1-\gamma_1}\left(\sqrt{1-\kappa_1}\ E_{in} + j\sqrt{\kappa_1}\ E_4\ e^{-\frac{\alpha}{2}\frac{L_D}{4} - jk_n\frac{L_D}{4}}\right) \quad (1)$$

$$E_{dr} = \sqrt{1-\gamma_3}\left(\sqrt{1-\kappa_3}\ E_{add} + j\sqrt{\kappa_3}\ E_2\ e^{-\frac{\alpha}{2}\frac{L_D}{4} - jk_n\frac{L_D}{4}}\right) \quad (2)$$

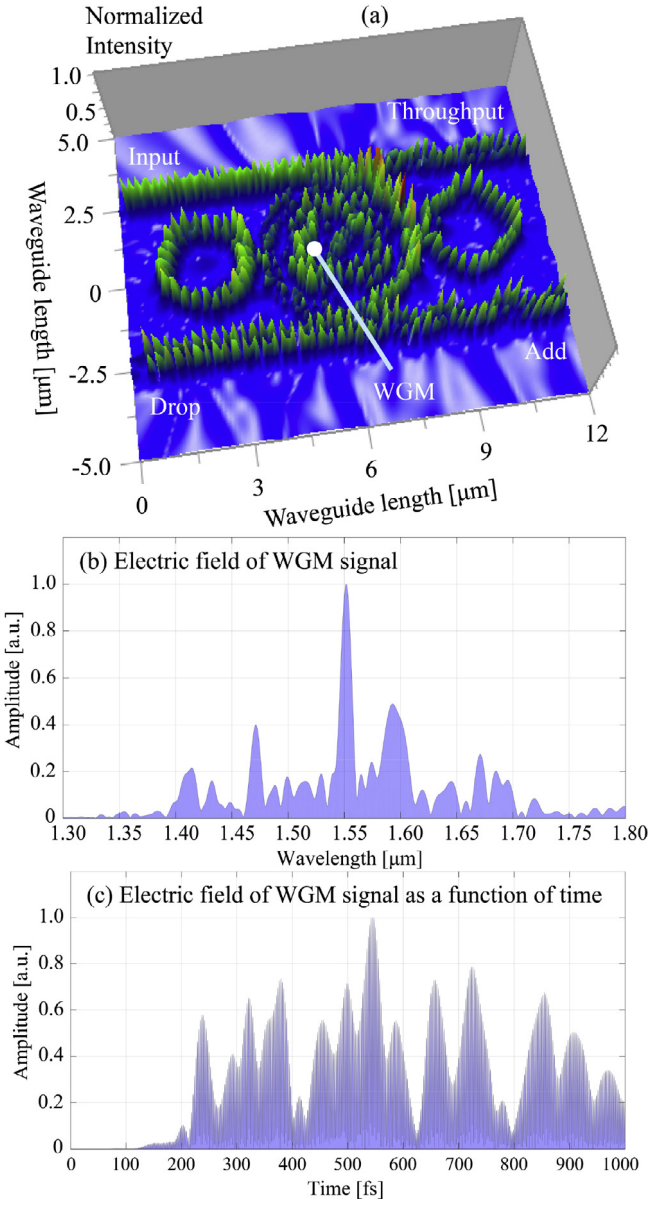

Fig. 2. Wave propagation results within the system shown in Fig. 1, where the input power is 2 W, and the center wavelength is 1.55 μm. The ring system, $\boldsymbol{R_L} = \boldsymbol{R_R} = 1.1\ \mu m$, $\boldsymbol{R_D} = 2.0\ \mu m$, $\boldsymbol{\kappa_1} = \boldsymbol{\kappa_2} = \boldsymbol{\kappa_3} = \boldsymbol{\kappa_4} = 0.5$, $\boldsymbol{n_{OChg}} = 2.9$, $\boldsymbol{n_{2ChG}} = 1.02 \times 10^{-17}\ m^2\ W^{-1}$ [25], $\boldsymbol{n_{Si}} = 3.47$ (Si-Crystalline silicon), where (a) the graphical results, (b) the electric field signal as a function of wavelength, and (c) the electric field signal as a function of time.

$$E_{out} = \sqrt{1-\gamma_3}\left(\sqrt{1-\kappa_3}\ E_{dr}^{*} + j\sqrt{\kappa_3}\ E_2\ e^{-\frac{\alpha}{2}\frac{L_D}{4} - jk_n\frac{L_D}{4}}\right) \quad (3)$$

Here, $\boldsymbol{E_{dr}^{*}} = -\boldsymbol{n}\boldsymbol{E_{dr}}$. n is the reflection ratio, E_{out} is the electric field output from the add port, E_1, E_2, E_3, and E_4 are the electric fields in the system. γ_{is} are the intensity insertion loss coefficients of the 3 dB couplers, and κ_{is} are the coupling constants. α is the attenuation loss of light in the waveguide, and $k_n = \frac{2\pi}{\lambda} n_{eff}$ is the propagation constant, L_D is the circumference of the center ring.

The suitable system parameters were achieved by using the graphical approach called the Optiwave program, from which the MATLAB program is used for numerical calculation. The parameters of the device are indicated in the figure captions. Fig. 1 shows the system, wherein the wave propagates within the system is shown in Fig. 2, where the Optiwave is used to perform the simulations. Here, the input power of 2 W at 1.55 μm is used. The ring radii are $\boldsymbol{R_L} = \boldsymbol{R_R} = 1.1\ \mu m$,

R_D = 2.0 μm. The coupling constants are κ_1 to κ_4 = 0.5, the refractive indices are n_{OChG} = 2.9, $n_{2ChG} = 1.02 \times 10^{-17}\,m^2\,W^{-1}$ [24,25], n_{Si} = 3.47 (Si-Crystalline silicon), where (a) the graphical results, (b) the electric field signal as a function of wavelength, and (c) the electric field signal as a function of time. The other parameters are given by the following details. We define the carrier density as n = [(Density) × (free electron number per atom) × (Avogadro's constant) × 10^6]/[Molar mass] electrons per cubic metre. For TiO_2, the density is 4.95 gcm^{-3}, the Avogadro's constant is 6.02×10^{23} atoms, the free electron number is 1, the Molar mass is 63.866 $gmol^{-1}$, and the conductivity, $\sigma = 2.38 \times 10^6\,Sm^{-1}$ [26]. Then the charge-carrier number density for the TiO_2 can be calculated as $n = [4.95 \times 1 \times (6.02 \times 10^{23}) \times 10^6]/63.866 = 4.6659 \times 10^{28}$ electrons-m^{-3}. The TiO_2 island radius(R_{TiO}) and thickness are 1.6 μm and 0.1 μm, respectively. The charge-carrier number can be calculated as $(4.6659 \times 10^{28}) \times \pi \times (1.6 \times 10^{-6})^2 \times (0.1 \times 10^{-6}) = 3.7525 \times 10^{10}$ electrons, where an electron itself has a negative charge of approximately 1.602×10^{-19} C [26]. Thus, the maximum electrical charge of the island is $Q_{max} = [3.7525 \times 10^{10}] \times [1.602 \times 10^{-19}] = 6.0115 \times 10^{-9}$ C. The charge in time on a system of two parallel conductive plates, which is a capacitor, can be calculated as the electric charge divided by the charging current. In addition, the current density, J, is the product between the electric field, E, inside the material and of which the conductivity, σ, that related to the material length (the thickness of the plate; T_{TiO}). Therefore, the charging current, I, can be calculated by $I = JA = \sigma T_{TiO} EA$, where $A = \pi[R_{TiO}]^2$ is the cross-section area of the material (area of the plates). In addition, the charge Q on a capacitor relates to the charging current I (coulombs^{-1}), which can be expressed as $Q = t \times I$, where t is the charging time. Therefore, the time-dependent charge of the capacitor in the plasmonic island can be considered as $Q(t) = [t \times \sigma T_{TiO} EA]$. The relationship of the charging Q as a function of time can be illustrated as in Fig. 3(a), in which the discharging time will depend on the applied loads. For simplicity, we suppose the plasmonic island charge is at the maximum(Q_{max}). The load driving current is the amount of Q per time, which is the electron source. Thus, the discharging Q as a function of time can be considered by $Q(t) = [Q_{max} - met]$, where m is an amount of discharging electron per time, e is the electron charge number approximately of 1.602×10^{-19} C, and t is time.

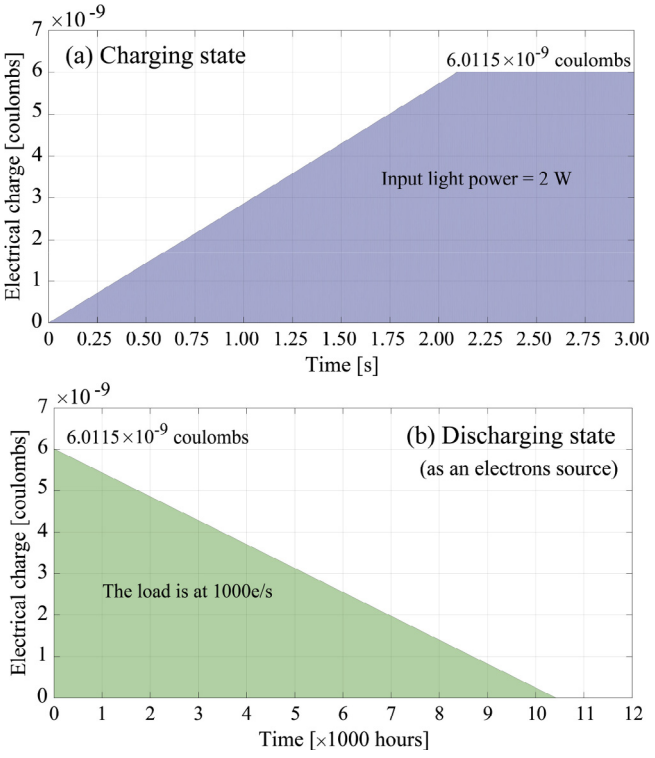

Fig. 3. Simulation result of the nano-capacitor-like characteristics using the system in Fig. 1, where (a) the charging state, where the input light power is at 2 W, and (b) the discharging state, where the applied load current is 1000 e/s.

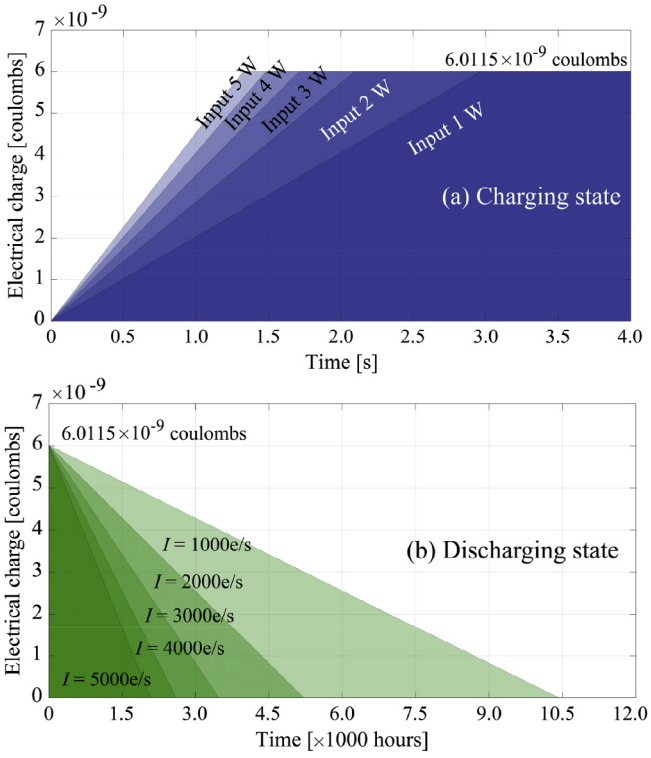

Fig. 4. Plots of the input power and charging and discharging time, where R_{TiO} = 1.6 μm and the thickness of each TiO_2 is 0.1 μm, and the titanium plate separation(d) is 0.2 μm. The applied load is varied from 1000 e/s to 5000 e/s, where (a) the charging state, (b) the discharging state. The charging time is less than 3 s in all cases, while the discharging time of 10, 000hours is obtained.

Similarly, the discharging state can be illustrated as in Fig. 3(b). Plots of the input power and charging and discharging time is shown in Fig. 4, where R_{TiO} = 1.6 μm, the reflector thickness(TiO_2) is 0.1 μm, and the TiO_2 plate separation(d) = 0.2 μm. The applied load is varied from 1000 e/s to 5000 e/s, where (a) the charging state, (b) the discharging state. The plot of the (stored) electron mobility in the island is shown in

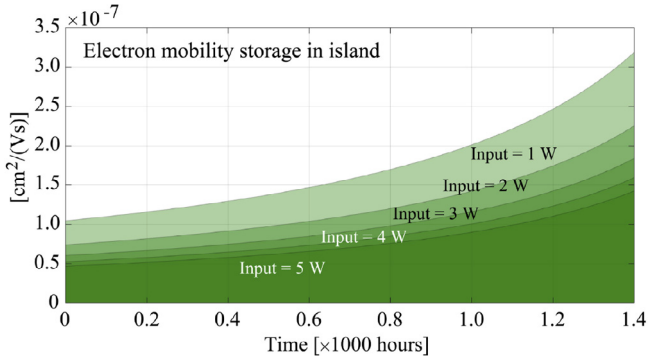

Fig. 5. Plot of the (stored) electron mobility in the island, where the load is drawn current is 1000 e/s from the island capacitor. The Titanium oxide layer parameters are R_{TiO} = 1.6 μm, thickness T_{TiO} = 0.1 μm. The electron mobility is $\mu = V_d/E$, where V_d is the drift velocity, which is $V_d = j_s/ne$, where $j_s = \sigma T_{TiO} E$ is the current density flowing through the material, e is the electron charge number, and n is the charge-carrier number density. The storage electron mobility can be reached the value of of 1.0×10^{-7} cm^2Â·Vs^{-1} within 15 min.

Fig. 5. For simplicity, we suppose that the load drawn current is 1000 e/s from the island capacitor, which corresponds to the amount of Q per time. The titanium oxide layer parameters are $R_{TiO} = 1.6$ μm, thickness $T_{TiO} = 0.1$ μm. In the calculation, the electron mobility, $\mu = V_d/E$, where V_d is the drift velocity, which is $V_d = j_s/ne$, where $j_s = \sigma T_{TiO} E$ is the current density flowing through the material, e is the electron charge number, and n is the charge-carrier number density (electrons per cubic metre). The stored electron mobility tends to increase when the electrons are drawn by the applied loads.

We have proposed the use of the capacitor-like circuit using the plasmonic island embedded microring system, which consists of a semi-closed microring resonator system. The input light energy is entered into the system and the successive pumping occurred. The charge process of the electron mobility is generated within the plasmonic island, which is formed by the capacitor-like circuit. By using the electro-optic energy conversion, the charge and discharge characteristics of the device are simulated and interpreted. The full electrical charge and discharge capacity can be achieved within 2–3 s and 1000 h, respectively, while the mobility discharge(emission) is controlled by the coated reflected end at the add port. The stored electron mobility within the island(nano-capacitor-like device) of 3.0×10^{-7} cm^2Vs^{-1} at 14,000 h is obtained. In application, the reflector at the drop port can be arranged to achieve the required discharge time and current. Additionally, the large volume of the circuits can be constructed and the more charge capacity values can be obtained, where the capacitors can be connected to form the circuits to obtain the higher capacitance. The device scale and materials can be found in the currently available materials, where the device scale can be supported by the current fabrication technology. The proposed system is almost a closed that can be used for the black-body radiation of the store energy, which may be useful for other investigations.

Acknowledgment

The authors would like to give the appreciation for the research financial support and the research facilities and financial support from the Universiti Teknologi Malaysia, Johor Bahru, Malaysia through Flagship UTM shine project (03G82), Tier 1 (16H44) and Tier 2 (15J57) grants. P. Yupapin would like to acknowledge for the research facilities from Ton Duc Thang University, Vietnam.

Appendix A. Supplementary material

Supplementary data associated with this article can be found, in the online version, at https://doi.org/10.1016/j.rinp.2018.07.013.

References

[1] Mitatha S, Kamoldilok S, Yupapin PP. White light generation and amplification using a soliton pulse within a nano-waveguide for potential of solar energy conversion use. Energy Convers Manage 2010;51:2340–4.
[2] Kamoldilok S, Yupapin PP. Nanoheat source generated by leaky light mode within a nano-waveguide for small electrical generator. Energy Convers. Manage. 2012;64:23–7.
[3] Srithanachai I, Uemmanapong S, Niemcharoen S, Yupapin PP. Novel design of solar cell efficiency improvement using an embedded electron accelerator on-chip. Opt Express 2012;20:12640–8.
[4] Ali J, Pornsuwancharoen N, Youplao P, et al. Coherent light squeezing states within a modified microring system. Results Phys 2018;9:211–4.
[5] Pornsuwancharoen N, Amiri IS, Suhailin FH, Aziz MS, Ali J, Singh G, Yupapin P. Micro-current source generated by a WGM of light within a stacked silicon-graphene-Au waveguide. IEEE Photon Technol Lett 2017;29:1768–71.
[6] Sasihithlu K, Dahan N, Greffet JJ. Light trapping in ultrathin CIGS solar cell with absorber thickness of 0.1 μm. IEEE J Photovoltaics 2018;8:621–5.
[7] Gupta ND, Janyani V. Lambertian and photonic light trapping analysis with thickness for GaAs solar cells based on 2D pereodic pattern. IET Optoelectron 2017;11:217–24.
[8] Goffard J, Colin C, Mollica F, Cattoni A, Sauvan C, et al. Light trapping in ultrathin CIGS solar cells with nanostructured back mirrors. IEEE J Photovoltaics 2017;7:1433–41.
[9] Gupta ND, Janyani V. Design and analysis of light trapping in thin film GaAs solar cells using 2-D photonic crystal structures at front surface. IEEE J Quantum Electron 2017;53:4800109.
[10] Nirmal A, Kyaw AKK, Jianxiong W, Dev K, Sun X, et al. Light trapping in inverted organic photovoltaics with nanoimprinted ZnO photonic crystal. IEEE J Photovoltaics 2017;7:545–9.
[11] Pornsuwancharoen N, Amiri IS, Suhailin FH, et al. Micro-current source generated by a WGM of light within a stacked silicon-graphene-Au waveguide. IEEE Photon Technol Lett 2017;29:1768–71.
[12] Ali J, Youplao P, Pornsuwancharoen N, et al. On-chip remote charger model using plasmonic island circuit. Results Phys 2018;9:815–8.
[13] Zainol FD, Jomtarak R, Daud D, Teeka C, Ali J, Yupapin PP. Atom bottom-up manipulation controlled by light for microbattery use. IEEE Trans Nanotechnol 2012;11:934–9.
[14] Gall D. Electron mean free path in elemental metals. J Appl Phys 2016;119:085101.
[15] Baccarani G, Ostoja P. Electron mobility empirically related to the phosphorus concentration in silicon. Solid-State Electron 1975;18:579–80.
[16] Sarapat N, Frank TD, Yupapin PP. Conjugate mirror design and simulation using a nonlinear coupling microring circuit. J. Nonlinear Opt Phys Mater 2013;22:1350024.
[17] Phatharacorn P, Chiangga S, Yupapin P. Analytical and simulation results of a triple micro whispering gallery mode probe system for a 3D blood flow rate sensor. Appl Opt 2016;55(33):009504.
[18] Pornsuwancharoen N, Youplao P, Amiri IS, Ali J, Yupapin P. Electron driven mobility model by light on the stacked metal–dielectric interfaces. Microwave Opt Technol Lett 2017;59:1704–9.
[19] Suwanarat S, Chiangga S, Amiri IS, et al. On-chip supercontinuum generation in nanostructured $Ge_{11.5}As_{24}Se_{64.5}$ chalcogenide waveguides using panda-ring. Results Phys 2018;10:38–44.
[20] Soysouvanh S, Jalil M, Amiri IS, et al. Ultra-fast electro-optic switching control using a soliton pulse within a modified add-drop multiplexer. Microsyst Technol 2018:1–6. Early Online.
[21] Chaiwong K, Tamee T, Punthawanunt S, et al. Naked-eye 3D imaging model using the embedded micro-conjugate mirrors within the medical micro-needle device. Microsyst Technol 2018;24:2695–9.
[22] Atabaki AH, Moazenni S, Pavanello F, et al. Integrating photonics with silicon nanoelectronics for next generation of system on a chip. Nature 2018;556:349–54.
[23] Koos C, Jacome L, Poulton C, et al. Nonlinear silicon-on-insulator waveguides for all-optical signal processing. Opt Express 2007;15:5976–90.
[24] Smektala F, Quemard C, Leneindre L, Lucas J, Barthélémy A, De Angelis C. Chalcogenide glasses with large non-linear refractive indices. J Non-Cryst Solids 1998;239:139–42.
[25] Mohr PJ, Newell DB, Taylor BN. CODATA recommended values of the fundamental physical constants. 2014. Rev Mod Phys 2016;88. 035009-1-73.
[26] Banus MD, Reed TB, Strauss AJ. Electrical and magnetic properties of TiO and VO. Phys Rev B 1972;5:2775.